



ELSEVIER

Available online at www.sciencedirect.com

SCIENCE @ DIRECT®

Journal of Magnetism and Magnetic Materials 305 (2006) 24–27

www.elsevier.com/locate/jmmm

Ferromagnetic resonance studies on $(\text{Co}_{40}\text{Fe}_{40}\text{B}_{20})_x(\text{SiO}_2)_{1-x}$ granular magnetic films

F. Yildiz^{a,b,*}, S. Kazan^c, B. Aktas^c, S.I. Tarapov^d, L. Tagirov^c, B. Granovsky^e^aDepartment of Physics, Faculty of Sciences and Arts, Celal Bayar University, Muradiye/Manisa, Turkey^bDepartment of Physics, Electron Spin Science Center, Pohang University of Science and Technology, Pohang 790-784, Republic of Korea^cGebze Institute of Technology, 41400 Gebze-Kocaeli, Turkey^dInstitute of Radiophysics and Electronics, National Academy of Sciences of Ukraine, Kharkov 61085, Ukraine^eMoscow State University, 119992 Moscow, Russian Federation

Received 13 June 2005; received in revised form 11 November 2005

Available online 12 December 2005

Abstract

Magnetic properties of granular $(\text{Co}_{40}\text{Fe}_{40}\text{B}_{20})_x(\text{SiO}_2)_{1-x}$ thin films ($x = 0.37 - 0.53$) have been studied by ferromagnetic resonance (FMR) technique. Samples have been prepared by ion-beam deposition of Co–Fe–B particles and SiO_2 on siall ceramic substrate. The FMR measurements have been done for different orientations of DC magnetic field with respect to the sample plane. It was found that the deduced value of effective magnetization from FMR data of the thin granular film is reduced by the volume-filling factor of the bulk saturation magnetization. The overall magnetization changes from 152 to 515 G depending on the ratio of the magnetic nanoparticles in the SiO_2 matrix. From angular measurements an induced in-plane uniaxial anisotropy has been obtained due to the preparation of the film conditions as well.

© 2005 Elsevier B.V. All rights reserved.

PACS: 75.30.Gw; 76.50.+g; 76.30.Fc

Keywords: Magnetic anisotropies; Ferromagnetic resonance; Granular magnetic films

1. Introduction

Magnetic and electrical properties of magnetic nanostructures are under intensive study now due to their promising technological applications such as magnetic data storage, extra-high-frequency (EHF) switches, etc. These nanostructures, either in nanolayered [1,2] or granular [3–5] form, show giant magnetic resistance (GMR) and giant magnetic impedance (GMI) effects. These phenomena reveal the remarkable change of resistance/impedance of the specimen at rather small applied static magnetic fields. Nanolayers have been studied more widely, since they could be approximated by the quasi-2D geometry. On

the other hand, the granular (quasi-3D) structures demonstrate a variety of properties, which cannot be explained using traditional approaches. In particular, they can be a basis for the manufacturing of 3D magneto-phonic crystals with electronically controlled properties [6]. For instance, they are promising to realize the “superprism effect” (electronically controlled forbidden zone) in 3D magneto-phonic crystal in the very high frequency band—closely to optical ones [7]. The advantage of 3D-structured crystals before standard ferromagnetic materials is that, a comparable small magnitude of static magnetic fields is enough to manipulate the magnetic permeability of Co–Fe–B granules drastically. Such properties seem to be quite profitable for application in spintronic technologies and particularly in EHF technologies, in the area of designing electronically managed devices due to the simplicity of the manufacturing technology of granular structures.

*Corresponding author. Department of Physics, Electron Spin Science Center, Pohang University of Science and Technology, Pohang 790-784, Republic of Korea. Tel.: +82 54 279 8383; fax: +82 54 279 8056.

E-mail address: fyildiz@gyte.edu.tr (F. Yildiz).

Therefore, intense attention is paid today to learn the magneto-refractive (MR) properties of granular nanostructures in optical and infrared frequency bands. More detailed research of these properties for ferromagnetic nanoparticles imbedded in an SiO_2 matrix for wavelength $\lambda = 5\text{--}20\ \mu\text{m}$ can be found particularly in Ref. [8]. Measurements of the present specimens for the millimeter waveband allowed to detect the GMI phenomena for this band [9]. This demonstrated the availability of these structures for EHF electronics and spintronics. Therefore, the detailed study of magnetic structures $\text{Co}_{40}\text{Fe}_{40}\text{B}_{20}$, which are given in the present work, is of great interest today.

2. Sample preparation and experimental technique

Samples have been prepared in Voronezh Technical University (Russia) by the YuKalinin team using the ion-beam deposition on sital ceramic substrate. The composite targets consist of the $\text{Co}_{40}\text{Fe}_{40}\text{B}_{20}$ alloy wafer, and silicon dioxide pieces on its surface were used for simultaneous co-deposition of the $(\text{Co}_{40}\text{Fe}_{40}\text{B}_{20})_x(\text{SiO}_2)_{1-x}$ granular film. The composition of the samples varied in the range of $x = 0.37\text{--}0.53$. The average size of metallic nanoparticles is in the range 2–5 nm, as determined from high-resolution electron microscopy [1]. The thickness of the specimens deposited on the glass ceramic is about 10 nm. Details of the sample preparation are described in Ref. [10]. The choice of the composition is determined by the fact that spin polarization of a CoFe alloy is greater than that of single Co and Fe. At the same time, the usage of SiO_2 as a matrix for systems with tunnel contacts allows to decrease the tunnel barrier that defines magneto-resistance [1].

The field derivatives of FMR spectra were taken by Bruker EMX electron spin resonance (ESR) spectrometer at the X-band frequency (9.5–9.8 GHz). The angular dependence of the ESR spectra was studied by varying the direction of the external magnetic field with respect to the film plane, both in the sample planes (in-plane geometry, IPG) and away from sample plane towards the film normal (out-of-plane geometry, OPG). The field derivative of microwave power absorption, dP/dH , was registered as a function of the magnetic field H .

3. Experimental results

Some selected ferromagnetic resonance spectra of the thin films are given in Fig. 1 for two extreme orientations of applied DC magnetic field H , namely parallel H_{\parallel} (solid line), and perpendicular H_{\perp} (dashed line) to the film plane. A single significantly broad and almost Lorentzian absorption has been observed in FMR spectra for all directions of the field. The slight deviation from Lorentzian shape could be attributed to the conduction properties of the film. As explained above, this conduction depends on the external field and, of course, relative orientations of the DC and AC field components. The external DC magnetic

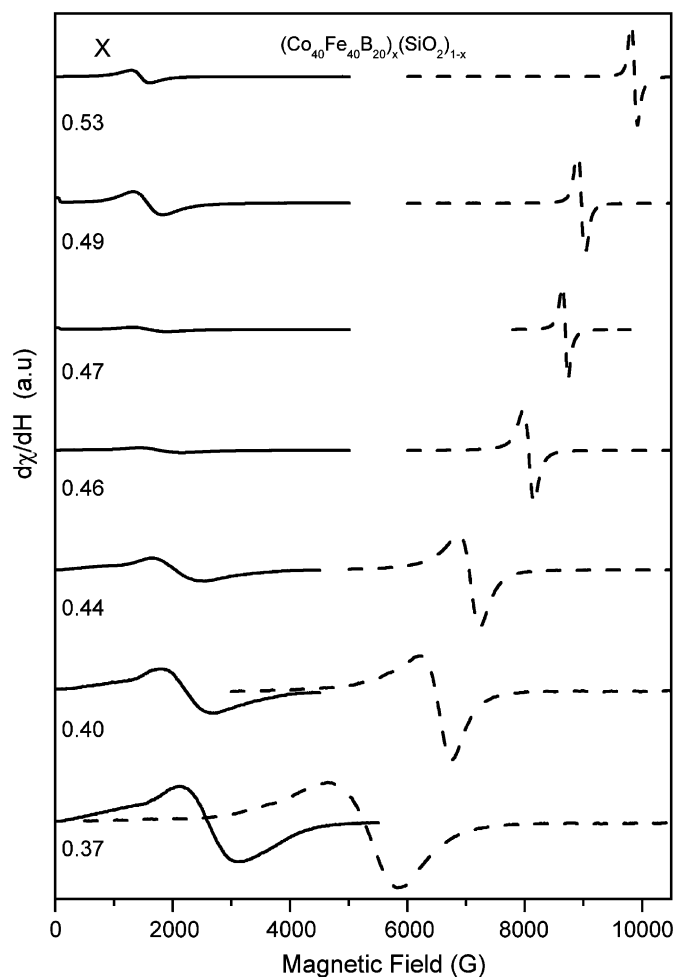


Fig. 1. FMR spectra of the $(\text{Co}_{40}\text{Fe}_{40}\text{B}_{20})_x(\text{SiO}_2)_{1-x}$ granular thin films. Solid lines belong to the IPG cases, dashed lines belong to the OPG cases.

field dependence of the theoretical magnetic susceptibility varies with the relative orientation of that vector as well. That is why the shape of the measured field derivative FMR spectra exhibit angular variation. The random orientation of intrinsic surface and shape anisotropies of nano-sized magnetic particles can contribute to the line width as well. On the other hand, depending on the sample preparation conditions, the so-called geometric (oblique) anisotropy manifests itself in a preferential direction, producing uniaxial in-plane anisotropy field.

Upon increasing the concentration of the $\text{Co}_{40}\text{Fe}_{40}\text{B}_{20}$ the resonance fields shift towards lower fields for the IPG case (solid line) and higher fields for the OPG case (dashed line) (see Fig. 1). It means that the overall magnetization increases with increasing ratio of the magnetic materials in the SiO_2 matrix. Line widths of the FMR spectra decrease with increasing $\text{Co}_{40}\text{Fe}_{40}\text{B}_{20}$ content because as the size of magnetic particles increase in the SiO_2 matrix, the magnetic ordering increases. The magnetic anisotropies due to the size effect and surface effect decrease and lead to narrowing of the FMR spectra. Angular dependence of the resonance field of the films for both in-plane and out-of-plane geometry is given in Figs. 2 and 3, respectively. As seen

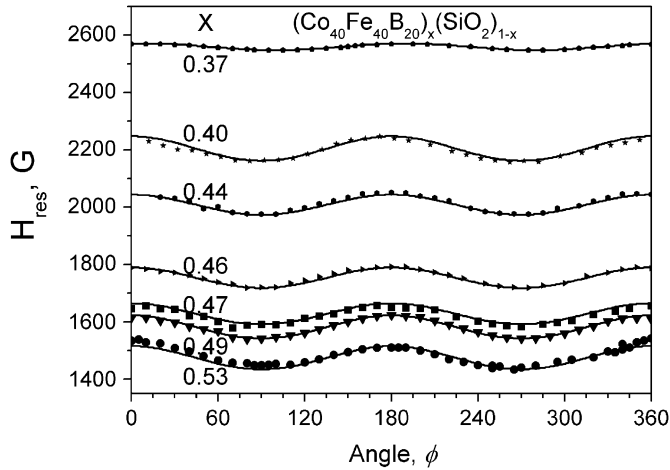


Fig. 2. Resonance field of the FMR spectra for the in-plane geometry. Solid lines are theoretical fitted curves, dots are experimental results.

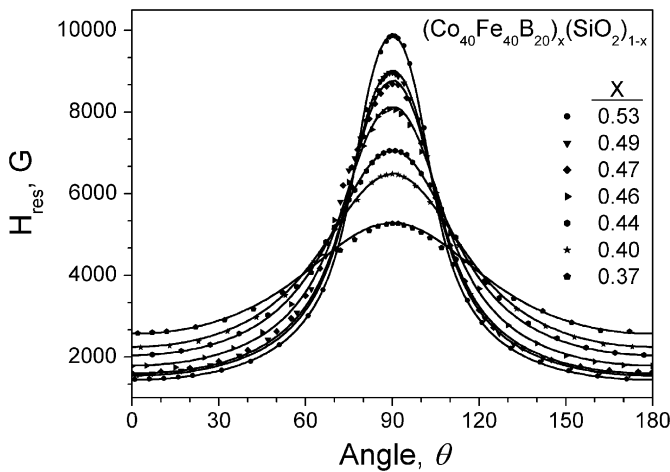


Fig. 3. Resonance field of the FMR spectra for the out-of-plane geometry. Solid lines are theoretical-fitted curves, dots are experimental results.

from Fig. 2 an in-plane uniaxial anisotropy has been observed from in-plane measurements. This anisotropy has been referred to the induced anisotropy which originates from preparation conditions of the films. Out-of-plane measurements (Fig. 3) imply demagnetization field growth progressively with increasing concentration of ferromagnetic nanoparticles.

4. Theoretical model and discussion

We have assumed the following magnetic free energy density:

$$E = -\vec{M} \cdot \vec{H} + 2\pi M^2 \cos^2 \theta + K_{ax} \sin^2 \theta \cos^2 \varphi \quad (1)$$

to calculate both FMR spectra and resonance field. Here, the first term represents the Zeeman energy of the film in the applied magnetic field (\vec{H}), the second term is the demagnetizing anisotropy energy and the last term represents assumed in-plane-induced uniaxial anisotropy

Table 1
Magnetic parameters of the $(\text{Co}_{40}\text{Fe}_{40}\text{B}_{20})_x(\text{SiO}_2)_{1-x}$ granular films

Concentration, x	M (G)	ω/γ (G)	K_{ax}/M (G)
0.53	515	3420	22
0.49	450	3380	22
0.47	430	3380	20
0.46	380	3380	20
0.44	294	3380	20
0.40	246	3410	25
0.37	152	3380	7

energy due to film preparation conditions. In Eq. (1) M and K_{ax} are the saturation magnetization and the axial anisotropy constant, respectively. The resonance condition for ferromagnetic resonance is given as [11]

$$\omega = \frac{\gamma}{M \sin \theta} \left[\frac{\partial^2 E}{\partial \theta^2} \frac{\partial^2 E}{\partial \varphi^2} - \left(\frac{\partial^2 E}{\partial \theta \partial \varphi} \right)^2 \right]^{1/2}, \quad (2)$$

where θ and φ are the equilibrium spherical angles for the static magnetization with respect to the reference axes, and they are determined by the zeros of the first derivatives of E with respect to the angle θ and φ . These values are used in Eq. (2) to determine the FMR resonance field H_{res} as a function of static magnetic field angles θ_H and φ_H for both IPG and OPG cases. The calculated resonance field values are plotted together with the experimental ones in Figs. 2 and 3. As seen from these figures, there are very good agreements between the experimental and simulated values for main modes. The determined magnetic properties of the granular films are given in Table 1. Actually, the deduced value for M also includes perpendicular uniaxial anisotropy field. However, since the analytical form of this anisotropy is completely identical to that of the demagnetizing field, it is impossible to separate this contribution from the magnetization by using the FMR experiment only. One needs an independent DC magnetization measurement to deduce the exact value for M . However, one does not expect the deduced value to be changed significantly because magneto-crystalline anisotropy should be much smaller compared to 6–10 kG. It should be noted that the deduced value for M is quite reasonable for this type of ferromagnetic structures.

One of the reasons of magnetic anisotropy in thin films is magnetic dipolar interaction which depends on the shape and boundaries of the sample. Normally, randomly distributed, amorphous, spherical, magnetic nanoparticles in an amorphous host material do not give any uniaxial anisotropy. The granular films were stripe-shaped (4–10 nm). In all films, the short side was the easy axis of magnetization, which is the initial direction of the ion beam while growing the film. Therefore, the uniaxial in-plane anisotropy is attributed to the preparation conditions.

Fig. 4 shows the values obtained from the theoretical fitting for magnetization against concentration of the

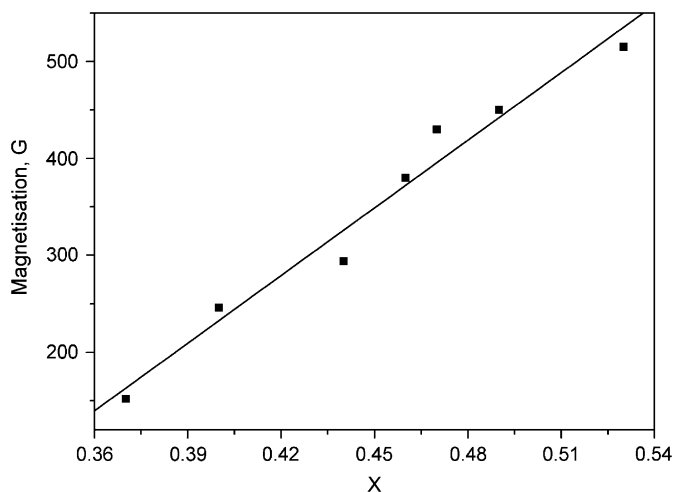


Fig. 4. Magnetization of the samples with respect to the concentration (x).

ferromagnetic component of the granular film. It should be noted that the overall macroscopic magnetization (effective magnetization of the film M_{eff}) in thin granular film form is reduced with respect to the bulk saturation magnetization (M_s) of the same materials by the volume-filling factor (f) of magnetic particles ($M_{\text{eff}} = M_s \cdot f$) in the non-magnetic matrix, as observed and discussed for various magnetic materials and a non-magnetic matrix in Ref. [12], and as given for iron and cobalt nanoparticles in polyimides in Ref. [13]. One can see from Fig. 4 that the concentration dependence can be fitted well by the linear function, with extrapolation to the bulk magnetization ($M_s \sim 1629$ G) of the same alloy.

5. Conclusion

Granular films $(\text{Co}_{40}\text{Fe}_{40}\text{B}_{20})_x(\text{SiO}_2)_{1-x}$ prepared on siall ceramic substrate by ion beam deposition method have been studied by FMR technique. Magnetic parameters of the films have been deduced with a theoretical model, and the bulk magnetization value of the $\text{Co}_{40}\text{Fe}_{40}\text{B}_{20}$ composite was determined. It is shown that the demagnetization fields have growth when the concentration of ferromagnetic nanoparticles in the films increase. The films have shown ferromagnetic behaviors consistently, with a filling factor of magnetic granular alloys in

the non-magnetic matrix. From in-plane FMR measurements an in-plane uniaxial anisotropy has been observed and referred to the non-spherical individual grains, whose long axes are preferentially oriented due to the film preparation conditions.

Acknowledgements

The work is supported by GYTE research fund with project number of 2003K and partially supported by STCU Grant no. 1916. Authors are grateful to Prof. Yu. Kalinin (Voronezh State University, Russia) for specimens performing and presentation, and to S. Nedukh and T. Bagmut for assistant in experiments.

References

- [1] A.S. Andreenko, V.A. Berezovec, A.B. Granovskij, *Fiz. Tverd. Tela* 45 (2003) 1446.
- [2] V.G. Kravets, D. Bozec, J.A.D. Matthew, S.M. Thompson, *J. Appl. Phys.* 91 (N10) (2002) 85.
- [3] P.M. Levy, *Solid State Phys.* 47 (1994) 367.
- [4] D.P. Belozorov, V.N. Derkach, S.V. Nedukh, A.G. Ravlik, S.T. Roschenko, I.G. Shipkova, S.I. Tarapov, F. Yildiz, B. Aktas, *J. Magn. Mater.* 263 (2003) 315.
- [5] O. Kohmoto, M. Munakata, N. Mineji, Y. Isagawa, *Mater. Sci. Eng. A* 375–377 (2004) 1069.
- [6] P.A. Belov, S.A. Tretyakov, A.J. Viitanen, *Phys. Rev. E* 66 (2002) 016608.
- [7] H. Kosaka, T. Kawashima, A. Tomita, M. Notomi, T. Tamamura, T. Sato, S. Kawakami, *Phys. Rev. B* 58 (1998) R10096.
- [8] A.B. Granovskij, I.V. Bykov, E.A. Gal'shina, V.S. Guschin, M. Inue, Yu.E. Kalinin, A.A. Kozlov, A.N. Yurasov, *JETP* 123 (N6) (2003) 1256.
- [9] S. Tarapov, T. Bagmut, A. Granovsky, V. Derkach, Yu. Kalinin, S. Nedukh, F. Yildiz, B. Aktas, L. Tagirov, *Proceedings of Fifth International Kharkov Symposium on Physics and Engineering of Microwaves, Millimeter and Submillimeter Waves, MSMW'2004, Kharkov, Ukraine, 2004*, pp. 751–753.
- [10] Yu.E. Kalinin, A.T. Ponomarenko, A.V. Sitnikov, et al., *Phys. Chem. Mater. Process.* 5 (2001) 14.
- [11] H. Suhl, *Phys. Rev.* 55 (1955) 555.
- [12] G.N. Kakazei, A.F. Kravets, N.A. Lesnik, M.M. Pereira deAzevedo, Yu.G. Pogorelow, J.B. Sousa, *J. Appl. Phys.* 85 (1999) 5654.
- [13] B.Z. Rameev, F. Yildiz, B. Aktas, C. Okay, R.I. Khaibullin, E.P. Zhglov, J.C. Pivin, L.R. Tagirov, *Microelectron. Eng.* 69 (2003) 330.